Cu(II) Binding to Monomeric, Oligomeric, and Fibrillar Forms of the Alzheimer's Disease Amyloid-β Peptide[†]

Jesse W. Karr[‡] and Veronika A. Szalai*

Department of Chemistry and Biochemistry, University of Maryland, Baltimore County, 1000 Hilltop Circle, Baltimore, Maryland 21250

Received December 11, 2007; Revised Manuscript Received February 27, 2008

ABSTRACT: Copper has been proposed to play a role in Alzheimer's disease through interactions with the amyoid-β (Aβ) peptide. The coordination environment of bound copper as a function of Cu:Aβ stoichiometry and Aβ oligomerization state are particularly contentious. Using low-temperature electron paramagnetic resonance (EPR) spectroscopy, we spectroscopically distinguish two Cu(II) binding sites on both soluble and fibrillar Aβ (for site 1, $A_{||} = 168 \pm 1$ G and $g_{||} = 2.268$; for site 2, $A_{||} = 157 \pm 2$ G and $g_{||} = 2.303$). When fibrils that have been incubated with more than 1 equiv of Cu(II) are washed, the second Cu(II) ion is removed, indicating that it is only weakly bound to the fibrils. No change in the Cu(II) coordination environment is detected by EPR spectroscopy of Cu(II) with Aβ (1:1 ratio) collected as a function of Aβ fibrillization time, which indicates that the Cu(II) environment is independent of Aβ oligomeric state. The initial Cu(II)−Aβ complexes go on to form Cu(II)-containing Aβ fibrils. Transmission electron microscopy images of Aβ fibrils before and after Cu(II) addition are the same, showing that once incorporated, Cu(II) does not affect fibrillar structure; however, the presence of Cu(II) appears to induce fibril-fibril association. On the basis of our results, we propose a model for Cu(II) binding to Aβ during fibrillization that is independent of peptide oligomeric state.

Alzheimer's disease (AD)[1] is a neurological disease that is the leading cause of dementia in elderly people, affecting roughly 15 million people in the world (*1*), 4.5 million of whom are Americans (*2*). Defining features of AD are the intra- and extracellular proteinaceous deposits linked to neuronal apoptosis (*3–5*). The major component of extracellular senile plaques in vivo is the 39–42-amino acid β-amyloid peptide (Aβ) (*6*). Metal ions, such as Cu(II) and Zn(II), are found in senile plaques (*7, 8*), and bind to Aβ in vitro (9–12), suggesting that metal ions play a role in AD etiology.

Copper in particular has been proposed to have a role in AD pathology (*9, 13–16*). Some reports find that Cu(II) acts as a neuroprotectant by preventing formation of toxic Aβ species (*17–20*), whereas others suggest that Cu(II) induces Aβ structures that are neurotoxic (*21, 22*). One proposal for explaining Aβ neurotoxicity induced by interaction with Cu(II) is that it results from changes in the Cu(II) coordination environment during Aβ oligomerization or as a function of Cu(II) concentration (*9, 23*). It is particularly important to characterize the coordination environment of Cu(II) with Aβ oligomers, an area that has not been explored in detail, given that Aβ oligomers are thought to be the principal neurotoxins in AD (*24–28*). Because copper also is implicated in AD etiology, unraveling the molecular level influence of copper on Aβ oligomerization is potentially important in understanding AD.

On the basis of current literature, soluble Aβ binds Cu(II) in a square planar coordination environment with predominantly nitrogen coordination (*14, 29, 30*). The number of nitrogen atom donors is at least three on the basis of simulation of an S-band EPR spectrum collected for Aβ with Cu(II) (*14*). This result led to the proposed three-nitrogen, one-oxygen (3N1O) coordination environment for Cu(II) bound to soluble Aβ. The general consensus is that most, if not all, of the nitrogen atom coordination comes from histidines at positions 6, 13, and 14 (*9, 13, 18, 30–34*). The amino terminus also has been proposed to coordinate the Cu(II) ion as one of the nitrogen atom donor ligands (*30, 32, 33*). Alternatively, Cu(II) has been proposed to bind Aβ via histidine and nonspecific interactions with residues 3–18 (*18*). The identity of the oxygen atom donor ligand has been debated extensively, with proposals ranging from tyrosine at position 10 (*9, 31*) to one of several possible carboxylate side chains (*33, 35, 36*). Far less work has focused on delineating the Cu(II) coordination environment in oligomeric and well-characterized fibrillar Aβ (*37, 38*).

To investigate the Cu(II) coordination environment in monomeric, oligomeric, and fibrillar Aβ40, we use low-

[†] Supported initially by an Alzheimer's Disease Research Pilot Project Award from the American Health Assistance Foundation (A2003-227) and currently by the Alzheimer's Association (IIRG-07-58211).

* To whom correspondence should be addressed. Phone: (410) 455-1576. Fax: (410) 455-2608. E-mail: vszalai@umbc.edu.

[‡] Current address: Department of Chemistry, Boston University, 590 Commonwealth Ave., Boston, MA 02215.

[1] Abbreviations: AD, Alzheimer's disease; Aβ, β-amyloid; EPR, electron paramagnetic resonance; ICP-MS, inductively coupled plasma mass spectrometry; ITC, isothermal titration calorimetry; NMR, nuclear magnetic resonance; TEM, transmission electron microscopy; HFIP, 1,1,1,3,3,3-hexafluoro-2-propanol; BSA, bovine serum albumin; PTA, phosphotungstic acid; ThT, thioflavin T.

10.1021/bi702423h CCC: $40.75
Published on Web 04/05/2008

temperature EPR spectroscopy in conjunction with microscopy and dye binding fluorescence assays. Our results lead us to propose a model for the involvement of Cu(II) in Aβ oligomerization in which 1 equiv of Cu(II) can bind at any point during the fibrillization process without affecting the resulting fibrillar morphology.

MATERIALS AND METHODS

Materials. Aβ40 and Aβ16 peptides were purchased from Bachem (King of Prussia, PA) or rPeptide (Athens, GA). The amino acid sequence for the Aβ40 peptide isDAEFRHDSGYEVHHQKLVFFAEDVGSNKGAIIGL-MVGGVV; the amino acid sequence of Aβ16 is the first 16 amino acids of Aβ40. Biological grade glycerol, sodium phosphate, 1,1,1,3,3,3-hexafluoro-2-propanol (HFIP), phosphotungstic acid (PTA), and sodium chloride were purchased from Fisher Scientific (Pittsburgh, PA). Bovine serum albumin (BSA) standards were purchased from Sigma-Aldrich (St. Louis, MO). Quartz EPR tubes were purchased from Wilmad (Buena, NJ). Carbon type-B 400 mesh copper grids were obtained from Ted Pella, Inc. (Redding, CA), and cross-ruled diffraction grating replicas were purchased from Structure Probe, Inc. (West Chester, PA). Solutions were prepared in MilliQ water (resistivity of >18 mΩ, total organic content of <35 ppb).

Sample Preparation. Aβ peptides were monomerized with HFIP and stored at −80 °C in HFIP as previously reported (*32, 38*). Peptide in HFIP was removed with a Hamilton gastight syringe that had been washed with multiple volumes of HFIP. An aliquot of the stock was removed for the determination of the peptide concentration using a BSA calibration curve (*32, 38*). Immediately prior to the use of peptide, HFIP was removed using a spin vacuum system. Preparation of samples by dissolution in HFIP followed by removal of HFIP produces homogeneous solutions of monomeric peptide (*39*).

Samples of soluble Aβ were prepared by resuspending dried peptide into buffer containing 50 mM NaP_i and 75 mM NaCl (pH 7.2). The Aβ16 peptide was used to model Cu(II) binding to soluble Aβ because it is well-established that this region contains the Aβ Cu-binding domain (*30–33*) and because it does not contain the fibrillization domain (residues 17–21) (*31*). Samples for EPR spectroscopy were prepared in buffer containing 50% glycerol (v/v). The use of glycerol as a cryoprotectant for biological samples is an accepted method for eliminating dipolar-induced broadening of EPR lines and for ensuring sample fidelity (*40, 41*). We have shown previously that inclusion of glycerol in solutions of Aβ does not affect the EPR properties of Cu(II) bound to Aβ40 fibrils (*38*).

Samples containing Aβ oligomers were prepared by incubating freshly resuspended Aβ40 peptide at 37 °C in 50 mM NaP_i and 75 mM NaCl (pH 7.2) with 50% glycerol (v/v) for 0–7 days under quiescent conditions in the absence of Cu(II). These samples were prepared in the presence of glycerol so that they could be directly transferred to EPR tubes following Cu(II) addition. Oligomeric species were not isolated prior to EPR data collection. Following the collection of EPR spectra for Aβ oligomers with Cu(II), thioflavin T (ThT) assays were performed to determine the β-sheet content in each sample (*42*).

Samples containing fibrils were prepared by incubating freshly resuspended Aβ40 peptide in 50 mM NaP_i and 75 mM NaCl (pH 7.2) at 37 °C for 7–14 days under quiescent conditions in the absence or presence of a stoichiometric amount of Cu(II). Samples were assayed for fibril formation by transmission electron microscopy (TEM) and ThT fluorescence (*32, 38, 42*). Fibrils for EPR experiments were separated by centrifugation in a microfuge (60 min, 16000 rcf), washed once with buffer, centrifuged a second time (30 min, 16000 rcf), and resuspended in 100 μL of 50 mM NaP_i and 75 mM NaCl (pH 7.2) containing 50% glycerol (v/v).

Cu(II) stock solutions were generated as previously reported (*32, 38, 43*). The Cu(II) concentration in each EPR sample was determined on the basis of a calibration curve generated from Cu(II)-glycine standards (molar ratio of 1:3) at pH 7.2 containing 75 mM NaCl and 50% glycerol (v/v). The concentration of Cu(II) in each of the Cu(II) EPR standards was assayed by chelation with bathocuproine disulfonic acid (BC) and reduction with ascorbate (*44*). The quantity of total copper as $[Cu(BC)_2]^{3-}$ was quantified at 483 nm [$\epsilon_{483} = 12500\ M^{-1}\ cm^{-1}$ (*44*)]. The 0, 25, 50, and 100 μM Cu(II) standards contained 0.4 ± 1.5, 27.7 ± 1.2, 54.1 ± 0.6, and 108.8 ± 0.7 μM Cu(II), respectively.

Electron Microscopy. Electron microscopy images were collected with a Zeiss-1OCA transmission electron microscope. Samples were placed on Carbon type-B 400 mesh copper grids and stained with 1% phosphotungstic acid (PTA). The actual magnification was within 90% of the magnification setting as determined by measuring the number of spaces within a fixed distance on commercially available cross-ruled diffraction grating replicas (*45*).

EPR Spectroscopy. EPR spectra were collected on a Bruker EMX 6/1 spectrometer equipped with a microwave frequency meter and an Oxford Instruments ESR900 liquid He cryostat system. All spectra were collected with the following experimental parameters: microwave frequency, 9.38 GHz; microwave power, 0.5 mW; modulation amplitude, 10 G; time constant, 40.96 ms; conversion time, 40.96 ms; gain, 5×10^4; eight scans; temperature, 20 K.

Addition of increasing amounts of Cu(II) to Aβ40 fibrils or Aβ16 (soluble) was performed on samples containing 100 μM peptide. Aliquots of a Cu(II) solution in MilliQ water were added to the sample in the EPR tube followed by mixing and refreezing to 77 K; the total volume change did not exceed 10%, and the total time for addition of Cu(II) and refreezing of the sample was approximately 2 min. At least three separate experiments were performed.

Thioflavin T Assay. Samples were assayed for β-sheet formation using the procedure previously reported (*32, 38, 42*). Briefly, 15 μL of sample was mixed with 3 mL of buffer containing 5 μM ThT in 50 mM glycine-NaOH (pH 8.5) (ThT assay buffer). Each sample was assayed in triplicate. Spectra were collected on a Jobin-Yvon Fluorolog-3 fluorometer using a 1 cm path length cuvette and the following conditions: wavelength range, 600–460 nm; integration time, 0.100 s; excitation slit width, 5 nm; emission slit width, 10 nm. The excitation wavelength was 446 nm, and spectra are an average of three scans.

RESULTS

A representative example of sequential addition of Cu(II) to metal-free Aβ40 fibrils is shown in Figure 1. The EPR spectrum of a substoichiometric amount of Cu(II) bound to

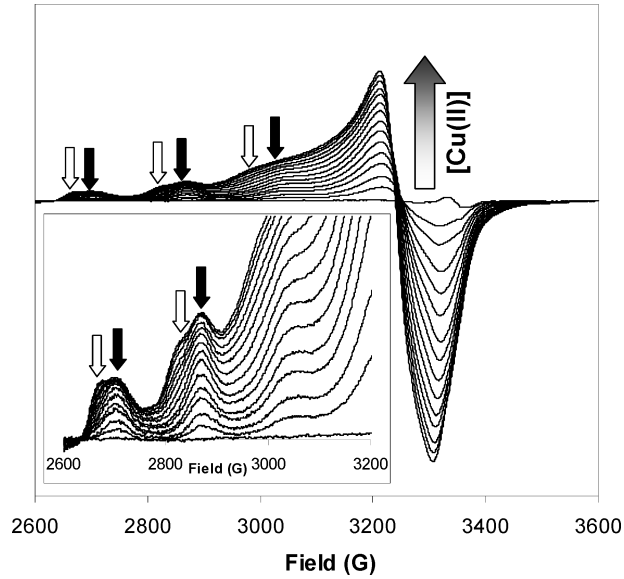

FIGURE 1: Representative EPR spectra recorded after addition of Cu(II) to fibrils formed from a solution of 100 μM Aβ40 in 50 mM NaP_i and 75 mM NaCl (pH 7.2) containing 50% glycerol (v/v). The inset shows the low field hyperfine peaks. Black arrows show hyperfine peaks positions for the high-affinity binding site, and white arrows show hyperfine peak positions for the low-affinity binding site.

Aβ40 fibrils and the measured EPR parameters for this Cu(II) species ($A_{||} = 168 \pm 1$ G, $g_{||} = 2.268 \pm 0.001$, $g_{||} = 2.061 \pm 0.002$) are similar to those reported previously (*32, 38, 46*). As the total amount of Cu(II) added increases above a stoichiometric equivalent, a second set of Cu(II) hyperfine peaks become evident (white arrows in Figure 1). This second set of hyperfine peaks has different EPR parameters ($A_{||} = 157 \pm 2$ G, $g_{||} = 2.303 \pm 0.008$, $g_{||} = 2.072 \pm 0.002$) than the first set. It also has different Cu(II) EPR parameters than component II in spectra of Cu(II) bound to the Aβ16D1N ($A_{||} = 156 \pm 1$ G, $g_{||} = 2.226$) (*43*) or Aβ2–16 mutants ($A_{||} = 153 \pm 3$ G, $g_{||} = 2.226$) (*32*). Additions were carried out to approximately 1.5–2.0 equiv of Cu(II) per peptide. The second Cu(II) ion is not retained when metal-free fibrils incubated with 1.2 or 2.6 equiv of Cu(II) are washed with buffer, resuspended, and re-evaluated by EPR spectroscopy; only Cu(II) in the first site remains bound (Figure 2). The second Cu(II) binding site was not created as a result of fibril formation because addition of Cu(II) to soluble Aβ16 yielded similar results (Figure S1 of the Supporting Information). Considering these results in conjunction with previous estimates of the affinity of Cu(II) for soluble Aβ in phosphate buffer (*10, 32*), we estimate that the binding affinity for Cu(II) bound in the first site on fibrils is in the micromolar range. We estimate that the second Cu(II) ion binds to fibrils with a much lower affinity (*36, 47*). Although a third Cu(II) ion might bind to Aβ because the peptide contains three histidine residues, we did not probe this possibility.

To test whether the temperature at which our samples are prepared influences the Cu(II) coordination environment in the first site, Cu(II) was added to Aβ40 that had been freshly dissolved in buffer at room temperature (RT) or at a low temperature (4 °C). At 4 °C, Aβ remains monomeric (*18, 19, 48*), but at higher temperatures, a mixture of Aβ species is present (*49–53*). We wanted to determine whether Cu(II) bound to this mixture of Aβ species has the same coordination

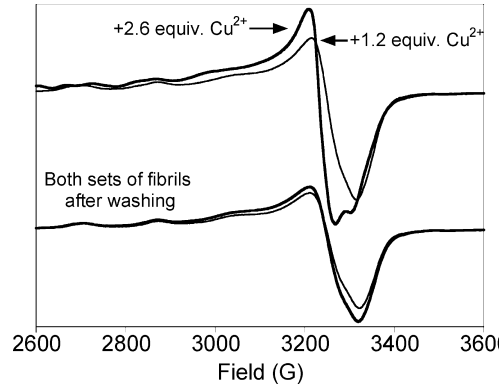

FIGURE 2: EPR spectra of two separate sets of fibrils isolated from metal-free solutions of 100 μM Aβ40 to which excess Cu(II) was added: thin line, 1.2 equiv of Cu(II) added; thick line, 2.6 equiv of Cu(II) added. Fibrils were removed from the sample tubes, centrifuged, and resuspended in 50 mM NaP_i and 75 mM NaCl (pH 7.2) containing 50% glycerol (v/v). EPR spectra collected postwashing show that only Cu(II) bound in the first Cu(II) site is retained.

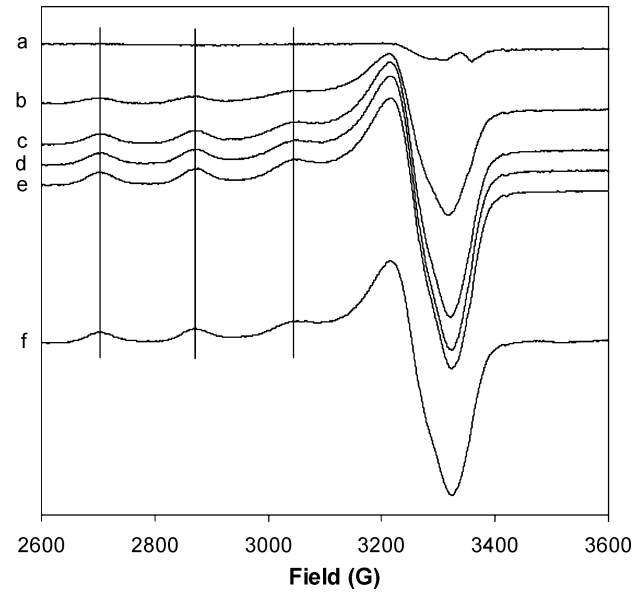

FIGURE 3: EPR spectra of soluble 100 μM Aβ40 with 1 equiv of Cu(II) prepared at 4 °C. (a) Soluble Aβ40 prepared at 4 °C in 50 mM NaP_i and 75 mM NaCl (pH 7.2) containing 50% glycerol (v/v). Spectrum b was recorded after addition of 1 equiv of Cu(II) at 4 °C to the sample used for spectrum a. Spectra c–e were recorded after 4 °C incubation of the sample used for spectrum b for an additional (c) 5, (d) 10, or (e) 240 min. (f) EPR spectrum of soluble Aβ40 with Cu(II) prepared at room temperature. Vertical lines show the alignment of hyperfine peaks.

environment as Cu(II) bound to exclusively monomeric Aβ prepared at 4 °C. EPR spectra for Cu(II) bound to soluble Aβ40 prepared at RT or 4 °C and frozen immediately are shown in Figure 3. EPR spectra for a sample containing Cu(II) bound to Aβ40 and incubated at 4 °C for a total of 4 h also are shown in Figure 3. The EPR spectrum of the Cu−Aβ40 sample prepared at RT is indistinguishable from that of the EPR spectrum of the Cu−Aβ40 sample prepared at 4 °C. The spectral features of Cu(II) bound to Aβ40 prepared and incubated at 4 °C do not change over the time period measured; however, the doubly integrated EPR spectral intensity (Figure S2 of the Supporting Information) for this sample increases in the first 10 min, signifying that Cu(II) binding to Aβ40 is slow at this temperature in our buffer. Note that after the initial 10 min period, the doubly integrated signal intensity remains

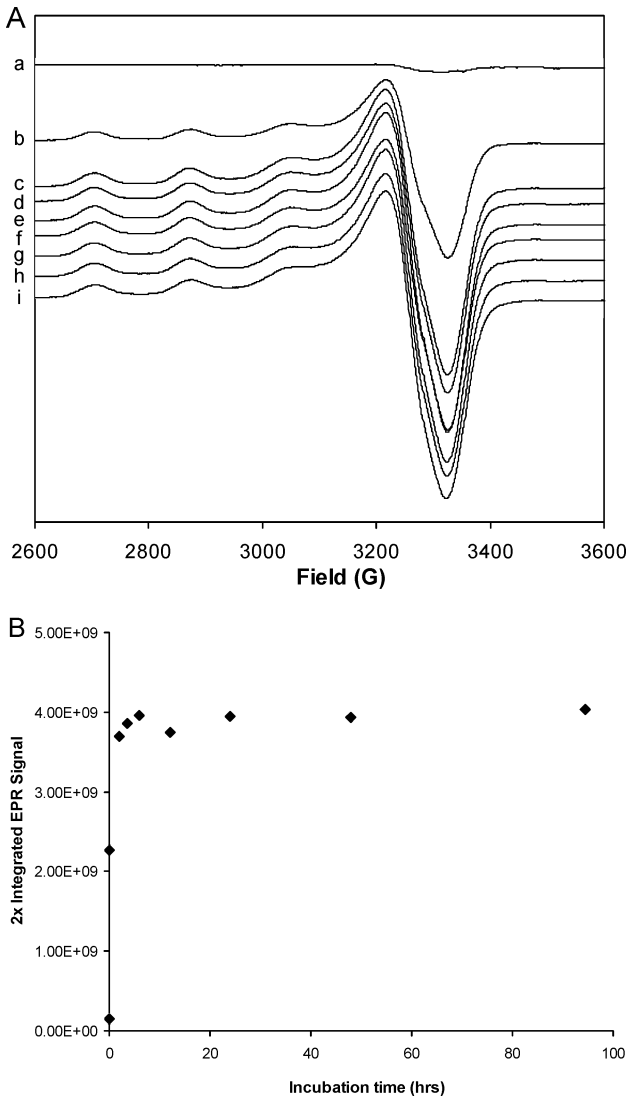

FIGURE 4: (A) EPR spectra of soluble 100 μM Aβ40 collected as a function of incubation time in the presence of Cu(II). Spectrum a is that of Aβ40 in 50 mM NaP_i and 75 mM NaCl (pH 7.2) containing 50% glycerol (v/v) before addition of 1 equiv of Cu(II). Spectrum b was recorded after addition of 1 equiv of Cu(II) and incubation for 2 min at RT. Spectra c–i were recorded following 37 °C incubation of the sample used for spectrum b for the following times: (c) 2, (d) 3.5, (e) 6, (f) 12, (g) 24, (h) 48, and (i) 94.5 h. Vertical lines show the alignment of hyperfine peaks. (B) Doubly integrated EPR signal intensity of spectra shown in panel A.

constant over the period of 6 h monitored by EPR spectroscopy. At the final time point (14 days), this sample shows increased ThT fluorescence (Figure S3 of the Supporting Information), confirming the presence of Aβ fibrils.

Previously published literature suggests that the Cu(II) coordination environment changes as a function of Aβ oligomeric state (*9, 31, 37*). Figure 4A shows EPR spectra of a stoichiometric amount of Cu(II) incubated with Aβ40 as a function of 37 °C incubation time. Cu(II) bound to Aβ40 at the first incubation time point represents Cu(II) bound to small oligomeric Aβ40 species, whereas each successive time point represents Cu(II) bound to a distribution of Aβ species with an increasing average size (gray arrow in Scheme 1). The measured EPR parameters for the initial Cu−Aβ40 spectrum are as follows: $A_{||} = 169$ G and $g_{||} = 2.265$. These parameters remain constant in each subsequent EPR spectrum. The doubly integrated signal intensity, which reflects

Scheme 1: Cu(II)−Aβ40 Oligomer Experimental Design[a]

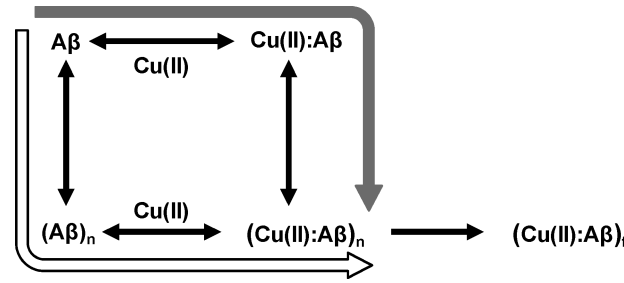

[a] The gray arrow depicts Cu(II) binding to Aβ prior to the formation of Aβ oligomers. The white arrow depicts the formation of metal-free Aβ oligomers to which Cu(II) was added. Note that both pathways result in formation of Cu(II)-containing Aβ fibrils. The distribution of oligomer sizes (or types) was not measured in our experiments.

the bound Cu(II) concentration, plateaus to a constant level (Figure 4B). After quiescent incubation at 37 °C for 7 days, a ThT assay confirmed the presence of β-sheet (Figure S4 of the Supporting Information), showing that the inclusion of a stoichiometric amount of Cu(II) in the fibrillizing Aβ40 solution does not prevent the formation of Aβ fibrils in our hands.

The previous experiment probed the Cu(II) coordination environment in solutions containing Aβ40 and Cu(II) from the outset of the experiment. In other words, oligomers are forming in the presence of Cu(II) during the incubation time. It is possible that oligomers generated in metal-free solutions of Aβ40 might bind Cu(II) differently than oligomers that form in the presence of Cu(II). Therefore, we investigated binding of a stoichiometric amount of Cu(II) to preformed metal-free Aβ40 oligomers. Aβ40 oligomers were prepared by 37 °C incubation of Aβ40 solutions without added Cu(II) for varying times (white arrow in Scheme 1). This preparation produces a distribution of metal-free Aβ species with an increasing average size over time (*49, 52, 53*) and allows us to probe the Cu(II) coordination environment of Aβ oligomers. Figure 5A shows the EPR spectra of Cu(II) bound to Aβ40 oligomers; the measured EPR parameters are listed in Table 1. A ThT assay confirms increasing β-sheet content in these samples as a function of oligomerization time (Figure S5 of the Supporting Information). Figure 5B shows EPR spectra of the Cu(II)-containing Aβ40 fibrils isolated from preformed metal-free Aβ oligomer samples to which Cu(II) was added. The measured EPR parameters for these fibrillar samples are listed in Table 2. The EPR spectra of Cu(II) bound to metal-free Aβ oligomers and the resulting fibrils show that Cu(II) binds to Aβ oligomers in a coordination environment that does not change. TEM images confirm the presence of fibrils after 7 days for each Aβ40 oligomer/Cu(II) sample (not shown).

TEM images in Figure 6 show the effect of addition of Cu(II) to metal-free Aβ40 fibrils. The metal-free fibrils were formed in 50 mM NaP_i and 75 mM NaCl (pH 7.2), and then Cu(II) was added to the fibrils. Images were collected at three different magnifications to show fibril characteristics. Panels A–C are the TEM images of the metal-free fibrils; panels D–F are the TEM images collected after addition of 1 molar equiv of Cu(II) to the fibrils. The measured widths for the metal-free Aβ fibrils and the Aβ40 fibrils after addition of Cu(II) are within error.

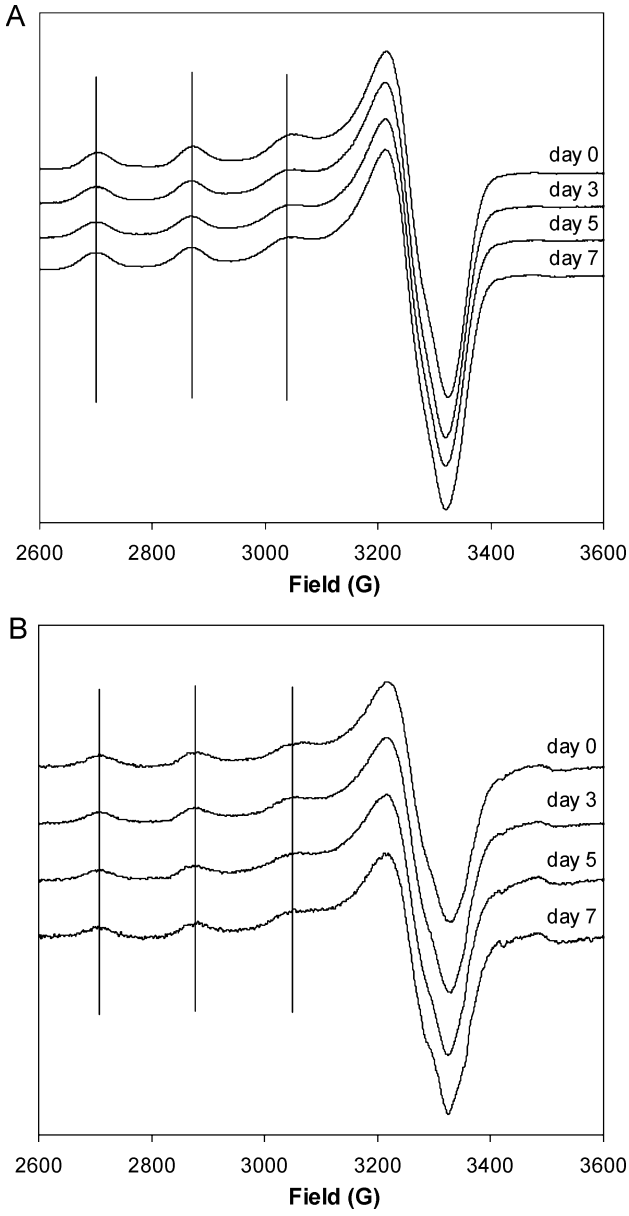

FIGURE 5: (A) EPR Spectra of 1 equiv of Cu(II) added to 100 μM metal-free Aβ40 oligomers prepared in 50 mM NaP_i and 75 mM NaCl (pH 7.2) containing 50% glycerol (v/v). Oligomers were prepared by quiescent 37 °C incubation of Aβ40 for 0, 3, 5, or 7 days prior to the addition of Cu(II). Samples were frozen to 77 K immediately after Cu(II) addition. (B) EPR Spectra of 1 equiv of Cu(II) added to 100 μM metal-free Aβ40 oligomers prepared in 50 mM NaP_i and 75 mM NaCl (pH 7.2) containing 50% glycerol (v/v) after 0, 3, 5, or 7 days and then incubated at 37 °C for a total of 7 days before isolation of fibrils. Vertical lines show the alignment of hyperfine peaks.

Table 1: Cu(II) EPR Parameters for Aβ40 Oligomeric Samples

sample	$A_{\|}$ (G)	$g_{\|}$	$g_{\perp}$
day 0	167 ± 1	2.266 ± 0.001	2.059
day 3	167 ± 2	2.267 ± 0.002	2.060
day 5	167 ± 2	2.269 ± 0.002	2.061
day 7	168 ± 2	2.269 ± 0.002	2.060

DISCUSSION

The majority of literature on Cu(II) binding to Aβ deals solely with binding to the soluble form of Aβ, with no reports characterizing the Cu(II) binding site(s) on Aβ fibrils or oligomers on the pathway to fibrils. Both fibrils (*54*) and oligomers (*22, 25–28, 55–57*) are neurotoxic. Here we report on Cu(II) binding to Aβ fibrils and are the first to show well-resolved EPR spectra that clearly illustrate two different Cu(II) binding sites on fibrils and soluble peptide. Although previous work has shown that 2 equiv of Cu(II) binds to Aβ (*30, 36, 58*), we present spectroscopic characterization of the distinct coordination environments of the two bound Cu(II) ions. The second Cu(II) binding site on Aβ fibrils is not created by the fibrillar architecture because Cu(II) EPR titrations of soluble Aβ16 show the same second Cu(II) binding site. Upon addition of >1 equiv of Cu(II) to Aβ, no change in the spectral features of the first Cu(II) binding site is observed. Deconvoluted EPR spectra for the first and second binding sites on Aβ indicate that the EPR spectrum of Cu(II) bound in the first site is unaffected by Cu(II) in the second binding site. This means that the Cu(II) coordination environment in the first site is not affected by the addition of excess Cu(II), an observation that is inconsistent with other work in which a broadened EPR spectrum is observed when >0.3 equiv of Cu(II) is added to soluble Aβ40 (*9*). Because those spectra were collected at higher temperatures, which decreases the signal-to-noise ratio in the spectra, it is possible that the broadened spectrum is due to incomplete resolution of the two sets of hyperfine peaks we observe or because the sample preparation and handling differ from our protocol.

Table 2: Cu(II) EPR Parameters for Aβ40 Fibrillar Samples

sample	$A_{\|}$ (G)	$g_{\|}$	$g_{\perp}$
day 0	171 ± 3	2.261 ± 0.003	2.059
day 3	166 ± 1	2.266 ± 0.001	2.059
day 5	167 ± 1	2.265 ± 0.001	2.061
day 7	170 ± 5	2.263 ± 0.006	2.061

Although there are some data on the affinity of Cu(II) for Aβ aggregates (*58*), to our knowledge, we are the first to probe Cu(II) bound to Aβ40 fibrils prepared in vitro and characterized by electron microscopy. We estimate that the two Cu(II) binding sites we observe by EPR spectroscopy have micromolar and millimolar binding affinities for both fibrillar and soluble Aβ (*10, 59*). This puts the binding affinity of the first Cu(II) site on Aβ40 fibrils in the range of previous reports of soluble Aβ40 for Cu(II) (*32*), whereas the second Cu(II) binding site has a much weaker affinity. These results corroborate isothermal titration calorimetry (ITC) work reported by Guilloreau et al. (*36*), who also observe high- and low-affinity (K_d values of 2×10^7 and 1×10^5 M^{-1}, respectively) Cu(II) binding sites for soluble Aβ16 and Aβ28.

A widespread controversy in the literature surrounds determination of the K_d of Cu(II) for Aβ. There are several methods that have been employed to determine this K_d, including tyrosine fluorescence quenching (*32, 60, 61*), ITC (*36, 62*), and competitive chelation assays combined with fluorescence (*30, 36, 63*). In the case of the ITC measurements in HEPES buffer by Guillereau et al. (*36*), the peptide concentration was 70 μM, which is much higher than the high-affinity K_d of 100 nM extracted from fits to the ITC data. Using competitive chelation and fluorescence, these authors observed that addition of histidine to the Cu(II)−Aβ complex recovered the quenched tyrosine fluorescence and concluded that this recovery was in line with the value of 10^7 M^{-1} determined by ITC. They

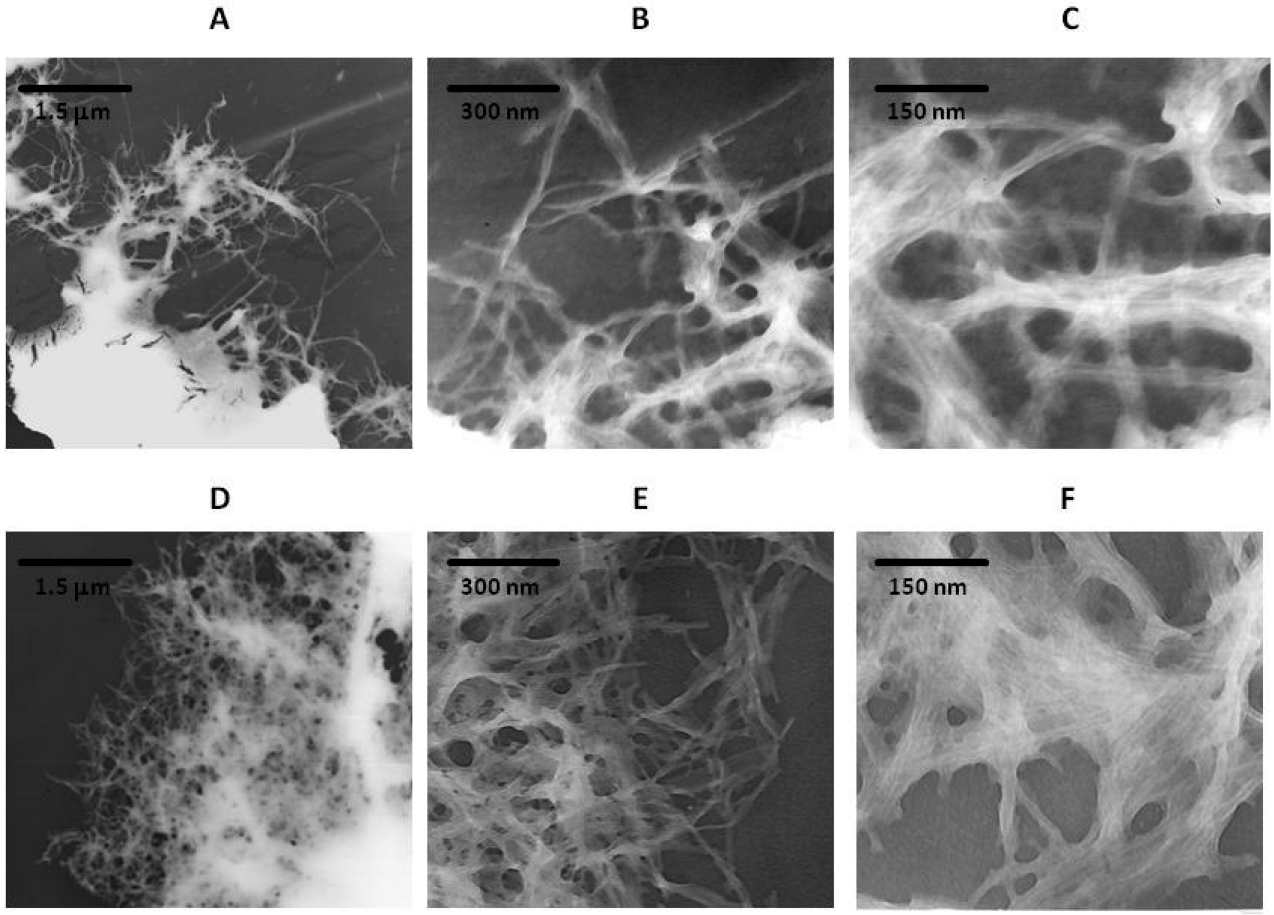

FIGURE 6: TEM images of fibrils formed from a solution of 100 μM Aβ40 in 50 mM NaP_i and 75 mM NaCl (pH 7.2) before (A−C) and after (D−F) Cu(II) addition. Samples were negatively stained with 1% phosphotungstic acid. Magnification: 10000× (A and D), 50000× (B and E), and 100000× (C and F).

observed the same effect upon addition of glycine to the Cu(II)−Aβ complex, which they state substantiates the K_d value for the low-affinity site they determined by ITC (*36*). Most recently, Talmard et al. (*62*) stated that the K_d of Cu(II) for Aβ is 1 μM in Tris buffer as measured by ITC. The Viles group (*30*) used competitive chelation fluorescence in *N*-ethylmorpholine buffer to determine the K_d of Cu(II) for Aβ16 and concluded that the K_d is between 10 and 100 nM. In the absence of buffers or salts, Ma et al. (*64*) obtained the same K_d range as Viles et al. (*30*) using an identical assay.

The measured affinity of metal ions for biomolecules depends heavily on the speciation of the metal ion in the medium. With respect to our work, Cu(II) binds to phosphate buffer, which means that Aβ competes with buffer for Cu(II) ions. Thus, although a micromolar K_d for the high-affinity site estimated from our EPR data is higher than that measured by other groups using competitive chelation or ITC, the interaction of Cu(II) with phosphate buffer suppresses binding to Aβ, which results in a higher apparent K_d. Our estimate of the high-affinity site K_d matches well with that measured by Garzon-Rodriguez et al. (*10*) and our own previous measurements (*32*) using direct tyrosine fluorescence quenching. Note that we use the estimated apparent affinities only as a means to compare the first and second sites on fibrillar and soluble peptide in our buffer medium. Because the composition of cerebral spinal fluid (CSF) is not well-modeled by buffer systems in which Cu−Aβ interactions have been investigated, the K_d values in the literature cannot be taken as equivalent to the K_d of Cu(II) for Aβ in vivo.

The second binding site for Cu(II) on Aβ is not revealed with every physical and analytical method used to probe binding. Recent mass spectrometry of Cu(II) bound to Aβ reported that only one Cu(II) ion binds to Aβ even when a 10-fold excess of Cu(II) is added to solutions of soluble Aβ (*47*). Likewise, previous fluorescence experiments used to determine the binding affinities of Cu(II) for Aβ did not indicate the presence of a second Cu(II) binding site (*32, 36*). One reason the low-affinity binding site might not have been detected is the fact that the ligands for the second Cu(II) ion are not derived exclusively from Aβ. Absorption spectra of Cu(II)-Aβ indicated that the second binding site has labile ligands (*36*). As noted by Guilloreau et al., this low-affinity binding site is most likely not relevant in vivo because the copper concentration in amyloid plaques is lower than that of Aβ. We note, however, that the total copper concentration in CSF is in the micromolar range (*8, 65–67*) and the Aβ concentration is in the nanomolar range (*50*), which means that during oligomerization the local copper:Aβ ratio might be higher than unity.

There have been conflicting reports about whether Cu(II) promotes or inhibits Aβ fibril formation. Here we show EPR spectra of Cu(II) bound to Aβ40 as a function of incubation time at 37 °C. These EPR spectra represent snapshots of the Cu(II)-containing oligomeric species formed during the

process of fibril formation. The Cu(II) EPR spectra do not change over time as the sample fibrillizes, indicating that the Cu(II) coordination environment does not change. The total concentration of copper bound to Aβ does not change during the oligomerization time which shows that as Aβ organizes into oligomers and then fibrils it retains Cu(II). Previous work from our laboratory has shown that fibrils formed in the presence of Cu(II) contain Cu(II) as determined by ICP-MS (*38*). For low-temperature EPR experiments, our samples contain glycerol, which has been reported to accelerate fibrillization kinetics without affecting fibril structure (*68*). We did not attempt to determine the kinetics of Aβ oligomerization in the presence of Cu(II), but rather the Cu(II) coordination environment as the oligomeric state of Aβ40 changes. At the end of the experiment, the presence of β-sheets was detected, consistent with Aβ fibril formation.

In our hands, Aβ40 incubated with a stoichiometric amount of Cu(II) consistently forms fibrils (*38*) rather than amorphous aggregates (*17, 18, 23, 37*). TEM images of Aβ40 fibrils before and after addition of 1 equiv of Cu(II) confirm that a stoichiometric Cu:peptide ratio does not disrupt fibril morphology. The average fibrillar widths of the metal-free and metal-containing fibrils are within error of each other, showing that binding of Cu(II) to Aβ fibrils does not drastically change the fibrillar structure (*38*). However, it does appear that the addition of Cu(II) causes some association of Aβ fibrils with each other. Fibril deposits appear to be more dense in samples that contain Cu(II), whereas the deposits in metal-free samples are more dispersed.

The observation that Cu(II) induces changes in fibril−fibril association has previously been reported with prion fibrils (*69*). Two possible scenarios could explain our observation of fibril−fibril association. The first is that fractional occupancy of Cu(II) in the low-affinity binding site induces cross-linking of Aβ fibrils through an interpeptide coordination mode. If this is the case, our Cu(II) EPR titrations showing the presence of the same second Cu(II) binding site on Aβ16 as on Aβ40 fibrils might mean that intermolecular Aβ association occurs at Cu:Aβ ratios of >1, consistent with other work (*31, 61, 70*). The second possible scenario is that binding of Cu(II) to metal-free Aβ fibrils in the high-affinity site increases the hydrophobicity of Aβ fibrils. Depending on the exact ligands from Aβ involved, binding of Cu(II) to the N-terminal region of Aβ might change its overall charge and/or structure, thereby slightly disrupting the structure of the N-terminal region of Aβ fibrils. Although it is widely agreed that the Cu(II) binding domain in Aβ is in the first 16 amino acids of the peptide sequence (*30–33*), the residue at which β-sheet propagation begins in Aβ40 fibrils is not (*71–74*). Thus, binding of Cu(II) at the N-terminus in Aβ fibrils might increase the hydrophobicity the Aβ fibrils, which in turn promotes fibril association as a means of reducing the solvent-exposed surface area. This proposal is significant because it means that Cu(II) could cause an increase in the local concentration of Aβ deposits through an indirect structural effect rather than through direct participation in peptide oligomerization and/or deposition.

Because the interstrand distance in β-sheets is 5 Å, one might expect Cu(II) ions to interact via dipolar coupling if each peptide in fibrils binds one high-affinity Cu(II) ion. It is well-established that Cu(II) binds to the N-terminal amino acids of Aβ. These same amino acids are solvent-exposed and structurally flexible in metal-free fibrils (*54, 75–78*). Therefore, one explanation for the lack of observation of dipolar interactions in Cu-containing fibril spectra is that the N-terminal regions of the fibrils splay apart to minimize electrostatic interactions when Cu(II) is bound. Another possibility is that the β-sheet of the fibrils "unzips" slightly to accommodate Cu(II) binding. Without further direct experimental information, it is difficult to speculate about the molecular structure of Cu-containing fibrils.

Initially, we used Aβ40 samples that were prepared at room temperature to monitor the Cu(II) coordination environment as a function of fibrillization. This protocol produces mixtures of Aβ species (*49, 52, 53*) rather than a homogeneous population of monomeric Aβ. To address this issue, we repeated the experiment using Aβ40 that had been prepared and handled at 4 °C, a protocol that produces monomeric peptide (*48*). When Cu(II) is added to Aβ40 at 4 °C, the Cu(II) EPR spectra look identical to those for peptide samples prepared at room temperature. These data indicate that the Cu(II) coordination environment in monomeric peptide and in a solution of peptide that contains a mixture of oligomers is the same.

A further question is whether Aβ oligomers bind Cu(II) differently than fibrillar or soluble Aβ, two species that have been characterized in detail by us and others (*14, 30–32, 38*). We conducted two different experiments to investigate this question (Scheme 1). First, we incubated Aβ40 with Cu(II) and collected EPR spectra as a function of time at 37 °C (gray arrow). In the second experiment, Aβ40 samples were preincubated at 37 °C and then Cu(II) was added (white arrow). Samples from this second type of experiment were either frozen directly after addition of Cu(II) or permitted to incubate for a total of 7 days prior to isolation of fibrils. The EPR spectra of all of these samples at all times points are spectroscopically similar with $g_{||}$ and $A_{||}$ values within error of each other. These results illustrate that the Cu(II) coordination environment is unaffected by the Aβ40 oligomeric state and that the Cu(II) binding is retained at all stages of the assembly process. Our data are consistent with recent NMR work showing Cu(II) remains bound to Aβ throughout the oligomerization process (*79*).

There are a number of models in the literature about the involvement of Cu(II) in Aβ oligomerization (*17–19, 23, 79–83*). Most authors report a decrease in the level of β-sheet formation by Aβ in the presence of Cu(II), as assayed by ThT fluorescence assays (*17–19, 37, 79, 83*). This decrease in the level of β-sheet formation in the presence of Cu(II) is explained by a model in which Cu(II) binding to monomeric Aβ creates a stable monomeric Cu−Aβ complex that does not progress to β-sheet-containing oligomers and/or fibrils (*18, 82, 83*). Hou et al. (*18*) additionally propose that when Cu(II) binds to preformed Aβ oligomers, the end point is nonfibrillar aggregates. As the Cu:Aβ ratio is increased above a stoichiometric level, several groups report that nonfibrillar intermediates and/or amorphous aggregates predominate (*23, 37, 83*). In contradiction to these reports, Zou et al. (*19*) found that at a 5:1 Cu(II):peptide ratio, all forms of in vitro aggregation of Aβ42 (to form fibrils or amorphous aggregates) are inhibited. A final proposed role for Cu(II) in the formation of Aβ oligomers is through formation of dityrosine cross-links via redox-mediated processes (*23,*

Scheme 2: Model for the Involvement of Cu(II) in Aβ Oligomerization and Fibrillization[a]

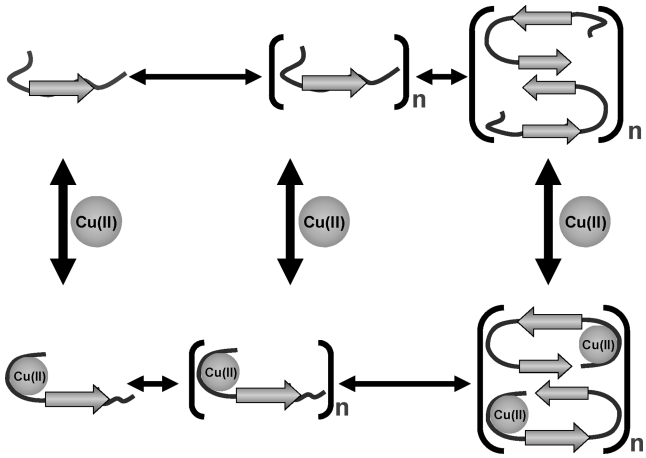

[a] The top pathway shows the oligomerization of monomeric Aβ into oligomers and then fibrils. The bottom pathway shows that Cu(II) binds to any of the metal-free Aβ species. No distinction between "prefibrillar" and "fibrillar" oligomers is made (*52, 53*).

80, 81). Clearly, a comprehensive description of the role of Cu(II) in Aβ aggregation is not yet available.

These seemingly conflicting models are not surprising given that different techniques provide information about discrete portions of the oligomerization mechanism. There is widespread disagreement in the literature regarding the treatments and conditions that provide the most reproducible results for association of metal-free Aβ (*39, 84–86*). A wide diversity of conditions is necessitated by each specific type of experiment, which could explain the disparate reports regarding fibril versus amorphous aggregate formation of Aβ in the presence of metal ions. If oligomers on the pathway to amorphous aggregates have a different molecular structure than oligomers resulting in fibrils and if the distribution of these two types of oligomers depends on factors other than the presence or concentration of copper, some of the conflicting reports in the literature could be explained.

Although consensus about how Cu(II) participates in Aβ oligomerization is not imminent, we propose a model to explain our finding that the Cu(II) coordination environment when bound to Aβ in phosphate buffer is invariant as a function of peptide oligomeric state (Scheme 2). We present two parallel paths representing the oligomerization process in the absence (top) and presence (bottom) of a stoichiometric amount of Cu(II). We show only a single population of oligomers in our model, but it is likely that more than one population is present (see below). A pathway to amorphous aggregates has not been included in our model. In the presence of Cu(II), the starting point is formation of a monomeric Cu−Aβ complex (*20, 82*). This Cu−Aβ monomer subsequently generates Cu(II)−Aβ oligomers that, under our conditions, ultimately lead to Cu(II)-containing fibrils (*38*). Incubation of solutions of Aβ lacking Cu(II) produces oligomers that also lead to fibrils (*51–53, 77, 87*). These metal-free oligomers can bind Cu(II) and proceed to make Cu(II)-containing fibrils. Finally, fibrils formed in the absence of Cu(II) can bind Cu(II) in the same coordination environment as that found for fibrils assembled in the presence of Cu(II), and the fibrils remain intact (*83*).

Our experimental data provide detailed information about the coordination environment of Cu(II) but do not provide direct information about the global oligomeric structure of Aβ adopted in the presence of Cu(II). Electron microscopy measurements demonstrate that Aβ40 fibrils form when Cu(II) is introduced at any time during the assembly process, which means that solutions containing Cu(II) and Aβ generate oligomers that can go on to fibrils. Recent work with oligomer-specific antibodies indicates there are two (or more) populations of oligomers that can go on to form fibrils (*27, 52, 53*). "Fibrillar oligomers" are monomers, dimers, and other oligomers that contain the same molecular-level structure as fully formed fibrils. A second population, called "prefibrillar oligomers", consists of oligomers that assemble and then undergo a conformational change prior to fibril formation. It is possible that addition of Cu(II) to solutions of metal-free Aβ changes the distributions of prefibrillar oligomers and fibrillar oligomers. In this regard, Cu(II) might prove to be a valuable probe if it induces a shift from one pathway to another. Talmard et al. (*82*) propose that formation of a monomeric Cu(II)−Aβ complex retards a key peptide conformational change required for formation of β-sheets. Although they did not characterize the aggregates (molecular mass of >75 kDa) they observed by EM or other methods that can detect β-sheets and/or fibrils, their results are consistent with Cu(II) participating in the fibrillar oligomer pathway (*52*), which consists of monomer−dimer and higher-molecular mass species (molecular mass of >50 kDa), but no intermediate-molecular mass species (*52*). Our results also suggest that Cu(II) might participate in a fibrillization pathway shift, but further work with samples containing predominantly prefibrillar or fibrillar oligomer populations along with detection of these populations using antibodies is required to fully test this hypothesis.

SUPPORTING INFORMATION AVAILABLE

EPR spectra for addition of Cu(II) to Aβ16, ThT assay and doubly integrated EPR signal intensity of Aβ40 with 1 equiv of Cu(II) as a function of 4 °C incubation, ThT assay data for an Aβ40 sample prepared at RT and incubated at 37 °C in the presence of Cu(II), and ThT assays of Aβ40 oligomers to which Cu(II) had been added. This material is available free of charge via the Internet at http://pubs.acs.org.

REFERENCES

1. Honig, L. S., and Mayeux, R. (2001) Natural history of Alzheimer's disease. *Aging (Milano, Italy) 13*, 171–182.
2. Hebert, L. E., Scherr, P. A., Bienias, J. L., Bennett, D. A., and Evans, D. A. (2003) Alzheimer disease in the US population: Prevalence estimates using the 2000 census. *Arch. Neurol. 60*, 1119–1122.
3. Behl, C. (2000) Apoptosis and Alzheimer's disease. *J. Neural. Transm. 107*, 1325–1344.
4. Engidawork, E., Gulesserian, T., Seidl, R., Cairns, N., and Lubec, G. (2001) Expression of apoptosis related proteins in brains of patients with Alzheimer's disease. *Neurosci. Lett. 303*, 79–82.
5. Loo, D. T., Copani, A., Pike, C. J., Whittemore, E. R., Walencewicz, A. J., and Cotman, C. W. (1993) Apoptosis is induced by β-amyloid in cultured central nervous system neurons. *Proc. Natl. Acad. Sci. U.S.A. 90*, 7951–7955.
6. Masters, C. L., Simms, G., Weinman, N. A., Multhaup, G., McDonald, B. L., Beyreuther, K., Roher, A. E., Chaney, M. O., Kuo, Y. M., Webster, S. D., Stine, W. B., Haverkamp, L. J., Woods, A. S., Cotter, R. J., Tuohy, J. M., Krafft, G. A., Bonnell, B. S., and Emmerling, M. R. (1985) Amyloid plaque core protein in Alzheimer disease and Down syndrome: Morphology and toxicity

of Aβ-(1–42) dimer derived from neuritic and vascular amyloid deposits of Alzheimer's disease. *Proc. Natl. Acad. Sci. U.S.A. 82*, 4245–4249.
7. Beauchemin, D., and Kisilevsky, R. (1998) A Method Based on ICP-MS for the Analysis of Alzheimer's Amyloid Plaques. *Anal. Chem. 70*, 1026–1029.
8. Lovell, M. A., Robertson, J. D., Teesdale, W. J., Campbell, J. L., and Markesbery, W. R. (1998) Copper, iron and zinc in Alzheimer's disease senile plaques. *J. Neurol. Sci. 158*, 47–52.
9. Curtain, C. C., Ali, F., Volitakis, I., Cherny, R. A., Norton, R. S., Beyreuther, K., Barrow, C. J., Masters, C. L., Bush, A. I., and Barnham, K. J. (2001) Alzheimer's Disease Amyloid-β Binds Copper and Zinc to Generate and Allosterically Ordered Membrane-penetrating Structure Containing Superoxide Dismutase-like Subunits. *J. Biol. Chem. 276*, 20466–20473.
10. Garzon-Rodriguez, W., Yatsimirsky, A. K., and Glabe, C. G. (1999) Binding of Zn(II), Cu(II), and Fe(II) ions to Alzheimer's disease Aβ peptide studied by fluorescence. *Bioorg. Med. Chem. Lett. 9*, 2243–2248.
11. Mantyh, P. W., Ghilardi, J. R., Rogers, S., DeMaster, E., Allen, C. J., Stimson, E. R., and Maggio, J. E. (1993) Aluminum, iron, and zinc ions promote aggregation of physiological concentrations of β-amyloid peptide. *J. Neurochem. 61*, 1171–1174.
12. Miura, T., Hori-i, A., Mototani, H., and Takeuchi, H. (1999) Raman spectroscopic study on the copper(II) binding mode of prion octapeptide and its pH dependence. *Biochemistry 38*, 11560–11569.
13. Atwood, C. S., Moir, R. D., Huang, X., Scarpa, R. C., Bacarra, N. M., Romano, D. M., Hartshorn, M. A., Tanzi, R. E., and Bush, A. I. (1998) Dramatic Aggregation of Alzheimer Aβ by Cu(II) is Induced by Conditions Representing Physiological Acidosis. *J. Biol. Chem. 273*, 12817–12826.
14. Huang, X., Cuajungco, M. P., Atwood, C. G., Hartshorn, M. A., Tyndall, J. D. A., Hanson, G. R., Stokes, K. C., Leopold, M., Multhaup, G., Goldstein, L. E., Scarpa, R. C., Saunders, A. J., Lim, J., Moir, R. D., Glabe, C., Bowden, E. F., Masters, C. L., Fairlie, D. P., Tanzi, R. E., and Bush, A. I. (1999) Cu(II) Potentiation of Alzheimer Aβ Neurotoxicity. *J. Biol. Chem. 274*, 37111–37116.
15. Huang, X., Atwood, C. G., Hartshorn, M. A., Multhaup, G., Goldstein, L. E., Scarpa, R. C., Cuajungco, M. P., Gray, D. N., Lim, J., Moir, R. D., Tanzi, R. E., and Bush, A. I. (1999) The Aβ Peptide of Alzheimer's Disease Directly Produces Hydrogen Peroxide through Metal Ion Reduction. *Biochemistry 38*, 7609–7616.
16. Opazo, C., Huang, X., Cherny, R. A., Moir, R. D., Roher, A. E., White, A. R., Cappai, R., Masters, C. L., Tanzi, R. E., Inestrosa, N. C., and Bush, A. I. (2002) Metalloenzyme-like Activity of Alzheimer's Disease β-Amyloid. *J. Biol. Chem. 43*, 40302–40308.
17. Yoshiike, Y., Tanemura, K., Murayama, O., Akagi, T., Murayama, M., Sato, S., Sun, X., Tanaka, N., and Takashima, A. (2001) New Insights on How Metals Disrupt Amyloid β-Aggregation and Their Effects on Amyloid-β Cytotoxicity. *J. Biol. Chem. 276*, 32293–32299.
18. Hou, L., and Zagorski, M. G. (2006) NMR reveals anomalous copper(II) binding to the amyloid Aβ peptide of Alzheimer's disease. *J. Am. Chem. Soc. 128*, 9260–9261.
19. Zou, J., Kajita, K., and Sugimoto, N. (2001) Cu^{2+} Inhibits the Aggregation of Amyloid β-Peptide(1–42) in vitro. *Angew. Chem., Int. Ed. 40*, 2274–2277.
20. Zou, K., Gong, J. S., Yanagisawa, K., and Michikawa, M. (2002) A novel function of monomeric amyloid β-protein serving as an antioxidant molecule against metal-induced oxidative damage. *J. Neurosci. 22*, 4833–4841.
21. Simmons, L. K., May, P. C., Tomaselli, K. J., Rydel, R. E., Fuson, K. S., Brigham, E. F., Wright, S., Lieberburg, I., Becker, G. W., Brems, D. N., Kirkitadze, M. D., Bitan, G., and Teplow, D. B. (1994) Secondary structure of amyloid β peptide correlates with neurotoxic activity in vitro Paradigm shifts in Alzheimer's disease and other neurodegenerative disorders: The emerging role of oligomeric assemblies. *Mol. Pharmacol. 45*, 373–379.
22. Kirkitadze, M. D., Bitan, G., and Teplow, D. B. (2002) Paradigm shifts in Alzheimer's disease and other neurodegenerative disorders: The emerging role of oligomeric assemblies. *J. Neurosci. Res. 69*, 567–577.
23. Smith, D. P., Ciccotosto, G. D., Tew, D. J., Fodero-Tavoletti, M. T., Johanssen, T., Masters, C. L., Barnham, K. J., and Cappai, R. (2007) Concentration Dependent Cu^{2+} Induced Aggregation and Dityrosine Formation of the Alzheimer's Disease Amyloid-β Peptide. *Biochemistry 46*, 2881–2891.
24. Lambert, M. P., Barlow, A. K., Chromy, B. A., Edwards, C., Freed, R., Liosatos, M., Morgan, T. E., Rozovsky, I., Trommer, B., Viola, K. L., Wals, P., Zhang, C., Finch, C. E., Krafft, G. A., and Klein, W. L. (1998) Diffusible, nonfibrillar ligands derived from $A\beta_{1-42}$ are potent central nervous system neurotoxins. *Proc. Natl. Acad. Sci. U.S.A. 95*, 6448–6453.
25. Cleary, J. P., Walsh, D. M., Hofmeister, J. J., Shankar, G. M., Kuskowski, M. A., Selkoe, D. J., and Ashe, K. H. (2005) Natural oligomers of the amyloid-β protein specifically disrupt cognitive function. *Nat. Neurosci. 8*, 79–84.
26. Walsh, D. M., Klyubin, I., Fadeeva, J. V., Cullen, W. K., Anwyl, R., Wolfe, M. S., Rowan, M. J., and Selkoe, D. J. (2002) Naturally secreted oligomers of amyloid β protein potently inhibit hippocampal long-term potentiation in vivo. *Nature 416*, 535–539.
27. Lesne, S., Koh, M. T., Kotilinek, L., Kayed, R., Glabe, C. G., Yang, A., Gallagher, M., and Ashe, K. H. (2006) A specific amyloid-β protein assembly in the brain impairs memory. *Nature 440*, 352–357.
28. Walsh, D. M., and Selkoe, D. J. (2007) Aβ oligomers: A decade of discovery. *J. Neurochem. 101*, 1172–1184.
29. Dong, J., Atwood, C. G., Anderson, V. E., Siedlak, S. L., Smith, M. A., Perry, G., and Carey, P. R. (2003) Metal Binding and Oxidation of Amyloid-β within Isolated Senile Plaque Cores: Raman Microscopic Evidence. *Biochemistry 42*, 2768–2773.
30. Syme, C. D., Nadal, R. C., Rigby, S. E. J., and Viles, J. H. (2004) Copper Binding to the Amyloid-β (Aβ) Peptide Associated with Alzheimer's Disease: Folding, Coordination Geometry, pH Dependence, Stoichiometry, and Affinity of Aβ-(1–28): Insights from a Range of Complementary Spectroscopic Techniques. *J. Biol. Chem. 279*, 18169–18177.
31. Miura, T., Suzuki, K., Kohata, N., and Takeuchi, H. (2000) Metal Binding Modes of Alzheimer's Amyloid β-Peptide in Insoluble Aggregates and Soluble Complexes. *Biochemistry 39*, 7024–7031.
32. Karr, J. W., Akintoye, H., Kaupp, L. J., and Szalai, V. A. (2005) N-Terminal Deletions Modify the Cu^{2+} Binding Site in Amyloid-β. *Biochemistry 44*, 5478–5487.
33. Kowalik-Jankowska, T., Ruta, M., Wisniewska, K., and Lankiewicz, L. (2003) Coordination abilities of the 1–16 and 1–28 fragments of β-amyloid peptide towards copper(II) ions: A combined potentiometric and spectroscopic study. *J. Inorg. Biochem. 95*, 270–282.
34. Zagorski, M. G., Yang, J., Shao, H., Ma, K., Zeng, H., and Hong, A. (1999) Methodological and Chemical Factors Affecting Amyloid β Peptide Amyloidogenicity. *Methods Enzymol. 309*, 189–204.
35. Rickard, G. A., Gomez-Balderas, R., Brunelle, P., Raffa, D. F., and Rauk, A. (2005) Binding Affinities for Models of Biologically Available Potential Cu(II) Ligands Relevant to Alzheimer's Disease: An ab Initio Study. *J. Phys. Chem. A 109*, 8361–8370.
36. Guilloreau, L., Damian, L., Coppel, Y., Mazarguil, H., Winterhalter, M., and Faller, P. (2006) Structural and thermodynamical properties of CuII amyloid-β16/28 complexes associated with Alzheimer's disease. *J. Biol. Inorg. Chem. 11*, 1024–1038.
37. Jun, S., and Saxena, S. (2007) The aggregated state of amyloid-β peptide in vitro depends on Cu^{2+} ion concentration. *Angew. Chem., Int. Ed. 46*, 3959–3961.
38. Karr, J. W., Kaupp, L. J., and Szalai, V. A. (2004) Amyloid-β binds Cu^{2+} in a mononuclear metal ion binding site. *J. Am. Chem. Soc. 126*, 13534–13538.
39. Stine, W. B., Jr., Dahlgren, K. N., Krafft, G. A., and LaDu, M. J. (2003) In vitro characterization of conditions for amyloid-β peptide oligomerization and fibrillogenesis. *J. Biol. Chem. 278*, 11612–11622.
40. Aronoff-Spencer, E., Burns, C. S., Avdievich, N. I., Gerfen, G. J., Peisach, J., Antholine, W. E., Ball, H. L., Cohen, F. E., Prusiner, S. B., and Millhauser, G. L. (2000) Identification of the Cu^{2+} Binding Sites in the N-Terminal Domain of the Prion Protein by EPR and CD Spectroscopy. *Biochemistry 39*, 13760–13771.
41. Weil, J. A., Bolton, J. R., and Wertz, J. E. (1994) *Electron Paramagnetic Resonance: Elementary Theory and Practical Applications*, Wiley, New York.
42. LeVine, H., III (1999) Quantification of β-sheet amyloid fibril structures with thioflavin T. *Methods Enzymol. 309*, 274–284.
43. Karr, J. W., and Szalai, V. A. (2007) Role of Aspartate-1 in Cu(II) Binding to the Amyloid-β Peptide of Alzheimer's Disease. *J. Am. Chem. Soc. 129*, 3796–3797.
44. Moffett, J., Zika, R. G., and Petasne, R. G. (1985) Evaluation of Bathocuproine for the Spectrophotometric Determination of Copper(I) in Copper Redox Studies with Applications in Studies of Natural Waters. *Anal. Chim. Acta 175*, 171–179.

45. Bozzola, J. J., and Russell, L. D. (1992) *Electron Microscopy: Principles and Techniques for Biologists*, Jones and Bartlett Publishers, Sudbury, MA.
46. Antzutkin, O. N. (2004) Amyloidosis of Alzheimer's Aβ Peptides: Solid-state nuclear magnetic resonance, electron paramagnetic resonance, transmission electron microscopy, scanning transmission electron microscopy and atomic force microscopy studies. *Magn. Reson. Chem. 42*, 231–246.
47. Jiang, D., Men, L., Wang, J., Zhang, Y., Chickenyen, S., Wang, Y., and Zhou, F. (2007) Redox Reactions of Copper Complexes Formed with Different β-Amyloid Peptides and Their Neuropathalogical Relevance. *Biochemistry 46*, 9270–9282.
48. Hou, L., Shao, H., Zhang, Y., Li, H., Menon, N. K., Neuhaus, E. B., Brewer, J. M., Byeon, I. J., Ray, D. G., Vitek, M. P., Iwashita, T., Makula, R. A., Przybyla, A. B., and Zagorski, M. G. (2004) Solution NMR studies of the Aβ(1–40) and Aβ(1–42) peptides establish that the Met35 oxidation state affects the mechanism of amyloid formation. *J. Am. Chem. Soc. 126*, 1992–2005.
49. Kusumoto, Y., Lomakin, A., Teplow, D. B., and Benedek, G. B. (1998) Temperature Dependence of Amyloid β-protein fibrillization. *Proc. Natl. Acad. Sci. U.S.A. 95*, 12277–12282.
50. LeVine, H., III (2004) Alzheimer's β-peptide oligomer formation at physiologic concentrations. *Anal. Biochem. 335*, 81–90.
51. Harper, J. D., Wong, S. S., Lieber, C. M., and Lansbury, P. T., Jr. (1999) Assembly of Aβ Amyloid Protofibrils: An in Vitro Model for a Possible Early Event in Alzheimer's Disease. *Biochemistry 38*, 8972–8980.
52. Kayed, R., Head, E., Sarsoza, F., Saing, T., Cotman, C. W., Necula, M., Margol, L., Wu, J., Breydo, L., Thompson, J. L., Rasool, S., Gurlo, T., Butler, P., and Glabe, C. G. (2007) Fibril specific, conformation dependent antibodies recognize a generic epitope common to amyloid fibrils and fibrillar oligomers that is absent in prefibrillar oligomers. *Mol. Neurodegener. 2*, 18.
53. Necula, M., Kayed, R., Milton, S., and Glabe, C. G. (2007) Small molecule inhibitors of aggregation indicate that amyloid β oligomerization and fibrillization pathways are independent and distinct. *J. Biol. Chem. 282*, 10311–10324.
54. Petkova, A. T., Leapman, R. D., Guo, Z., Yau, W. M., Mattson, M. P., and Tycko, R. (2005) Self-Propagating, Molecular-Level Polymorphism in Alzheimer's β-Amyloid Fibrils. *Science 307*, 262–265.
55. Glabe, C. G. (2006) Common mechanisms of amyloid oligomer pathogenesis in degenerative disease. *Neurobiol. Aging 27*, 570–575.
56. Townsend, M., Shankar, G. M., Mehta, T., Walsh, D. M., and Selkoe, D. J. (2006) Effects of secreted oligomers of amyloid β-protein on hippocampal synaptic plasticity: A potent role for trimers. *J. Physiol. 572*, 477–492.
57. Demuro, A., Mina, E., Kayed, R., Milton, S. C., Parker, I., and Glabe, C. G. (2005) Calcium dysregulation and membrane disruption as a ubiquitous neurotoxic mechanism of soluble amyloid oligomers. *J. Biol. Chem. 280*, 17294–17300.
58. Atwood, C. S., Scarpa, R. C., Huang, X., Moir, R. D., Jones, W. D., Fairlie, D. P., Tanzi, R. E., and Bush, A. I. (2000) Characterization of copper interactions with alzheimer amyloid β peptides: Identification of an attomolar-affinity copper binding site on amyloid β1–42. *J. Neurochem. 75*, 1219–1233.
59. Connors, K. A. (1987) *Binding Constants*, 1st ed., John Wiley & Sons, New York.
60. Garzon-Rodriguez, W., Yatsimirsky, A. K., and Glabe, C. G. (1999) Binding of Zn(II), Cu(II), and Fe(II) Ions to Alzheimer's Aβ Peptide Studied by Fluorescence. *Bioorg. Med. Chem. Lett. 9*, 2243–2248.
61. Danielsson, J., Pierattelli, R., Banci, L., and Graslund, A. (2007) High-resolution NMR studies of the zinc-binding site of the Alzheimer's amyloid β-peptide. *FEBS J. 274*, 46–59.
62. Talmard, C., Bouzan, A., and Faller, P. (2007) Zinc Binding to Amyloid-β: Isothermal Titration Calorimetry and Zn Competition Experiments with Zn Sensors. *Biochemistry 46*, 13658–13666.
63. Ma, Q. F., Hu, J., Wu, W. H., Liu, H. D., Du, J. T., Fu, Y., Wu, Y. W., Lei, P., Zhao, Y. F., and Li, Y. M. (2006) Characterization of copper binding to the peptide amyloid-β(1–16) associated with Alzheimer's disease. *Biopolymers 83*, 20–31.
64. Ma, Q.-F., Hu, J., Wu, W.-H., Liu, H.-D., Du, J.-T., Fu, Y., Wu, Y.-W., Lei, P., Zhao, Y.-F., and Li, Y.-M. (2006) Characterization of Copper Binding to the Peptide Amyloid-β(1–16) Associated with Alzheimer's disease. *Biopolymers 83*, 20–31.
65. Berthon, G., Matuchansky, C., and May, P. M. (1980) Computer Simulation of Metal Ion Equilibria in Biofluids. Part 3. Trace Metal Supplementation in Total Parenteral Nutrition. *J. Inorg. Biochem. 13*, 63–73.
66. Hershey, C. O., Hershey, L. A., Varnes, A., Vibhakar, S. D., Lavin, P., and Strain, W. H. (1983) Cerebrospinal fluid trace element content in dementia: Clinical, radiologic, and pathologic correlations. *Neurology 33*, 1350–1353.
67. Palm, R., Strand, T., and Hallmans, G. (1986) Zinc, total protein, and albumin in CSF in patients with cerebrovascular diseases. *Acta Neurol. Scand. 74*, 308–313.
68. Yang, D. S., Yip, C. M., Huang, T. H., Chakrabartty, A., and Fraser, P. E. (1999) Manipulating the Amyloid-β Aggregation Pathway with Chemical Chaperones. *J. Biol. Chem. 274*, 32970–32974.
69. Bocharova, O. V., Breydo, L., Salnikov, V. V., and Baskakov, I. V. (2005) Copper(II) inhibits in vitro conversion of prion protein into amyloid fibrils. *Biochemistry 44*, 6776–6787.
70. Ali, F. E., Separovic, F., Barrow, C. J., Yao, S., and Barnham, K. J. (2006) Copper and zinc mediated oligomerisation of Ab peptides. *Int. J. Pept. Res. Ther. 12*, 153–164.
71. Petkova, A. T., Ishii, Y., Balbach, J. J., Antzutkin, O. N., Leapman, R. D., Delaglio, F., and Tycko, R. (2002) A structural model for Alzheimer's β-amyloid fibrils based on experimental constraints from solid state NMR. *Proc. Natl. Acad. Sci. U.S.A. 99*, 16742–16747.
72. Petkova, A. T., Yau, W. M., and Tycko, R. (2006) Experimental constraints on quaternary structure in Alzheimer's β-amyloid fibrils. *Biochemistry 45*, 498–512.
73. Tycko, R., and Ishii, Y. (2003) Constraints on supramolecular structure in amyloid fibrils from two-dimensional solid-state NMR spectroscopy with uniform isotopic labeling. *J. Am. Chem. Soc. 125*, 6606–6607.
74. Shivaprasad, S., and Wetzel, R. (2004) An Intersheet Packing Interaction in Aβ Fibrils Mapped by Disulfide Cross-Linking. *Biochemistry 43*, 15310–15317.
75. Kheterpal, I., Williams, A., Murphy, C., Bledsoe, B., and Wetzel, R. (2001) Structural Features of the Aβ Amyloid Fibril Elucidated by Limited Proteolysis. *Biochemistry 40*, 11757–11767.
76. Whittemore, N. A., Mishra, R., Kheterpal, I., Williams, A. D., Wetzel, R., and Serpersu, E. H. (2005) Hydrogen-Deuterium (H/D) Exchange Mapping of $A\beta_{1-40}$ Amyloid Fibril Secondary Structure Using Nuclear Magnetic Resonance Spectroscopy. *Biochemistry 44*, 4434–4441.
77. Tycko, R. (2004) Progress towards a molecular-level structural understanding of amyloid fibrils. *Curr. Opin. Struct. Biol. 14*, 96–103.
78. Torok, M., Milton, S., Kayed, R., Wu, P., McIntire, T., Glabe, C. G., and Langen, R. (2002) Structural and dynamic features of Alzheimer's Aβ peptide in amyloid fibrils studied by site-directed spin labeling. *J. Biol. Chem. 277*, 40810–40815.
79. Lim, K. H., Kim, Y. K., and Chang, Y.-T. (2007) Investigations of the Molecular Mechanism of Metal-Induced Aβ(1–40) Amyloidogenesis. *Biochemistry 46*, 13523–13532.
80. Atwood, C. G., Perry, G., Zeng, H., Kato, Y., Jones, W. D., Ling, K.-Q., Huang, X., Moir, R. D., Wang, D., Sayre, L. M., Smith, M. A., Chen, S. G., and Bush, A. I. (2004) Copper Mediates Dityrosine Cross-Linking of Alzheimer's Amyloid-β. *Biochemistry 43*, 560–568.
81. Barnham, K. J., Haeffner, F., Ciccotosto, G. D., Curtain, C. C., Tew, D., Mavros, C., Beyreuther, K., Carrington, D., Masters, C. L., Cherny, R. A., Cappai, R., and Bush, A. I. (2004) Tyrosine gated electron transfer is key to the toxic mechanism of Alzheimer's disease β-amyloid. *FASEB J. 18*, 1427–1429.
82. Talmard, C., Guilloreau, L., Coppel, Y., Mazarguil, H., and Faller, P. (2007) Amyloid-β peptide forms monomeric complexes with Cu(II) and Zn(II) prior to aggregation. *ChemBioChem 8*, 163–165.
83. Raman, B., Ban, T., Yamaguchi, K. I., Sakai, M., Kawai, T., Naiki, H., and Goto, Y. (2005) Metal ion-dependent effects of clioquinol on the fibril growth of an amyloid β peptide. *J. Biol. Chem. 280*, 16157–16162.
84. Wood, S. J., Maleeff, B., Hart, T., and Wetzel, R. (1996) Physical, Morphological and Functional Differences between pH 5.8 and 7.4 Aggregates of the Alzheimer's Amyloid Peptide Aβ. *J. Mol. Biol. 256*, 870–877.
85. Chen, Y. R., and Glabe, C. G. (2006) Distinct early folding and aggregation properties of Alzheimer amyloid-β peptides Aβ40 and Aβ42: Stable trimer or tetramer formation by Aβ42. *J. Biol. Chem. 281*, 24414–24422.

86. Mamikonyan, G., Necula, M., Mkrtichyan, M., Ghochikyan, A., Petrushina, I., Movsesyan, N., Mina, E., Kiyatkin, A., Glabe, C. G., Cribbs, D. H., and Agadjanyan, M. G. (2007) Anti-A β 1–11 antibody binds to different β-amyloid species, inhibits fibril formation, and disaggregates preformed fibrils but not the most toxic oligomers. *J. Biol. Chem. 282*, 22376–22386.

87. Kirschner, D. A., Inouye, H., Duffy, L. K., Sinclair, A., Lind, M., and Selkoe, D. J. (1987) Synthetic peptide homologous to β protein from Alzheimer disease forms amyloid-like fibrils in vitro. *Proc. Natl. Acad. Sci. U.S.A. 84*, 6953–6957.

BI702423H